Raman Scattering in the Mott Insulators $LaTiO_3$ and $YTiO_3$: Evidence for Orbital Excitations

C. Ulrich,[1] A. Gössling,[2] M. Grüninger,[2] M. Guennou,[1] H. Roth,[2] M. Cwik,[2] T. Lorenz,[2] G. Khaliullin,[1] and B. Keimer[1]

[1]*Max-Planck-Institut für Festkörperforschung, Heisenbergstrasse 1, D-70569 Stuttgart, Germany*

[2]*II. Physikalisches Institut, Universität zu Köln, 50937 Köln, Germany*

(Received 28 February 2005; published 9 October 2006)

Raman scattering is used to observe pronounced electronic excitations around 230 meV—well above the two-phonon range—in the Mott insulators $LaTiO_3$ and $YTiO_3$. Based on the temperature, polarization, and photon energy dependence, the modes are identified as orbital excitations. The observed profiles bear a striking resemblance to magnetic Raman modes in the insulating parent compounds of the superconducting cuprates, indicating an unanticipated universality of the electronic excitations in transition metal oxides.

DOI: 10.1103/PhysRevLett.97.157401 PACS numbers: 78.30.Hv, 71.28.+d, 75.50.Dd, 75.50.Ee

Transition metal oxides with orbital degeneracy exhibit a host of intriguing physical properties, such as ''colossal magnetoresistance'' in manganites or unconventional superconductivity in ruthenium oxides [1,2]. Collective oscillations of the valence electrons between different atomic orbitals (termed ''orbitons'') contain a wealth of information about the microscopic interactions underlying this behavior. Experiments introducing Raman scattering as a direct probe of orbitons in $LaMnO_3$ have hence opened up new perspectives for a quantitative understanding of colossal magnetoresistance [3]. The results, however, have proven to be quite controversial, because the modes observed in $LaMnO_3$ are difficult to discriminate from ordinary two-phonon excitations [4,5].

Insulating titanates such as $LaTiO_3$ and $YTiO_3$ have only one valence electron residing on the Ti^{3+} ions. Despite their similar, nearly cubic lattice structures, the magnetic ground states of $LaTiO_3$ and $YTiO_3$ are quite different: Whereas $LaTiO_3$ orders antiferromagnetically at $T_N \sim 150$ K, $YTiO_3$ is a ferromagnet with Curie temperature $T_C \sim 30$ K. The origin of this difference lies in the large degeneracy of the quantum states available to the valence electron. In addition to its spin degeneracy, this electron can occupy any combination of the three t_{2g} orbitals xy, xz, and yz. The six single-ion states on neighboring sites are coupled by the superexchange interaction and collective lattice distortions, which generate a plethora of nearly degenerate many-body states with different spin and orbital ordering patterns.

The mechanisms selecting the ground state out of this manifold of states have recently been a focus of intense research. Two theoretical approaches have emerged. According to point charge model [6–8], band structure [9,10], and local-density approximation–dynamical mean-field theory [11] calculations, the degeneracy of the single-ion t_{2g}-levels is lifted by subtle lattice distortions. The calculated orbital patterns have received support from NMR [12,13] and neutron diffraction [14] experiments. However, some aspects of the magnetic order and dynamics appear difficult to reconcile with the scenario of static, lattice-driven orbital order [15,16]. An alternative theoretical approach [17,18] emphasizes the collective quantum dynamics of the orbitals, driven by intersite superexchange interactions. Frustrations inherent to these interactions give rise to strong quantum fluctuations that suppress orbital ordering and stabilize more isotropic charge distributions around the Ti^{3+} ions.

Orbital excitations have the potential to discriminate between these conflicting scenarios. When the orbital dynamics is quenched by lattice distortions, one expects a number of transitions between well-defined crystal field levels, with selection rules dictated by the symmetry of these distortions. The picture is similar to the local crystal field excitations of, e.g., Ti^{3+} impurities in a distorted corundum lattice [19]. In an orbitally fluctuating state, on the other hand, the orbital excitations are collective modes with selection rules controlled by many-body effects and hence are very different from local crystal field excitations. Therefore, the observation of orbital excitations and comparison of their properties in $YTiO_3$ and $LaTiO_3$, two materials with different lattice distortions and magnetic ground states, is of crucial importance for the understanding of this hotly debated issue.

We have used Raman scattering to search for orbital excitations in pure and lightly oxygen doped $LaTiO_{3+\delta}$, and in pure $YTiO_3$. The samples were high quality single crystals with $T_N = 146$ K, $T_N = 120$ K, and $T_C = 27$ K, respectively, grown by the floating zone technique described in Ref. [6]. The $LaTiO_3$ crystal was partly twinned. Raman measurements were performed using a Dilor-XY triple spectrometer equipped with a CCD detector. The measured spectral intensity was calibrated by using a white light source (Ulbricht-sphere) as reference. In order to avoid heating of the sample, the power of the incident laser beam was kept below 10 mW at the sample position. The experiments were performed in backscattering geometry parallel to the crystallographic b direction (within the $Pbnm$ space group). The polarizations of the incident and scattered photons are specified as (z, z), (x, z), etc., where $z \parallel c$ is along the nearest-neighbor Ti-Ti bond whereas x is along the next-nearest-neighbor Ti-Ti direc-

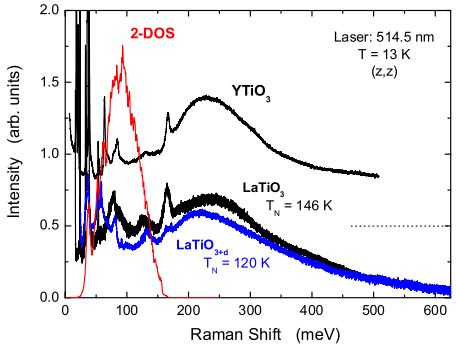

FIG. 1 (color online). Raman spectra of $LaTiO_3$, $LaTiO_{3+\delta}$, and $YTiO_3$ measured at $T = 13$ K using the 514.5 nm laser line of an Ar^+/Kr^+ mixed gas laser. The data on $LaTiO_{3+\delta}$ were taken on a fully twinned sample, and the intensity was normalized based on the polarization dependence determined for $LaTiO_3$ (Fig. 4). The red line shows the calculated two-phonon density of states.

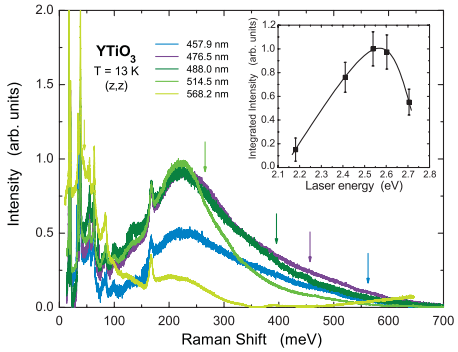

FIG. 2 (color). Raman spectrum of $YTiO_3$ measured at $T = 13$ K for different laser lines. A frequency independent background has been subtracted from every profile. The arrows depict the position of the photoluminescence peak at 2.14 eV for the different laser lines. The inset shows the integrated intensity of the broad high-energy peak.

tion in the ab plane. The z' and x' directions are rotated by 45° from z and x.

Figure 1 shows the Raman spectra of $LaTiO_3$ and $YTiO_3$ over a wide energy range. Up to 80 meV, the spectra are dominated by one-phonon excitations reported before [20,21]. A series of weak features extends up to 170 meV. At still higher frequencies, around 235 meV, a pronounced broad peak is observed in both compounds [22]. The latter feature has hitherto not been reported and constitutes the central observation of this Letter.

In order to establish whether the broad peak can be attributed to two-phonon excitations, we have evaluated the two-phonon density of states (2-DOS) of $YTiO_3$ by convoluting the one-phonon dispersion curves calculated within a shell model whose parameters were fitted to the observed phonon frequencies [23]. The 2-DOS, responsible for the weak features between 80 and 170 meV, terminates at about 170 meV. The broad peak thus occurs well above the two-phonon spectral range, in contrast to the features around 160 meV discussed for $LaMnO_3$ [3,4]. Since higher phonon orders are expected to appear even weaker, lattice vibrations can be ruled out as the origin of the high-energy Raman peak. As an aside, we note the presence of a sharp feature at the upper edge of the 2-DOS around 165 meV, which is not reproduced by our calculation. This peak is also observed by inelastic neutron scattering [23]. A similar Raman mode is also observed in other transition metal oxides [3,20,24,25], and has been attributed to a two-phonon excitation [4,20,24,25].

In order to rule out photoluminescence as a cause of the broad peak, we have repeated the Raman measurements with different laser lines between 457.9 nm and 568.2 nm (Fig. 2). The peak at 235 meV does not shift as the laser frequency is changed, ruling out photoluminescence as the origin and demonstrating that the peak position corresponds to a genuine excitation energy. The data also show the manifestations of a weak photoluminescence feature of energy 2.14 eV and width 75 meV, which is responsible for the low-energy intensity in the data at the laser wavelength 568.2 nm. For the other spectra, the luminescence peak is shifted with respect to the laser line, and therefore contributes to the variation of the apparent line shape of the 235 meV mode with laser wavelength. However, the main part of the mode profile is unaffected by this extraneous feature. The inset of Fig. 2 shows that the integrated spectral weight of the 235 meV mode in $YTiO_3$ exhibits a pronounced resonant enhancement at a laser frequency of ~2.54 eV. The Raman spectra displayed in Fig. 3 demonstrate that its spectral weight is also strongly temperature dependent, decreasing continuously with increasing temperature.

For the investigation of the influence of oxygen defects on the Raman intensity, we have repeated the experiment on $LaTiO_{3+\delta}$ samples whose Néel temperatures are reduced by a significant oxygen nonstoichiometry. Representative data are shown in Fig. 1. For this sample, the background in the Raman spectrum at low energies close to the laser line is larger than in the insulating samples, probably due to luminescence or Raman scattering on free charge carriers [26]. The broad feature at high energies, on the other hand, remains almost unchanged. This demonstrates that the broad feature does not arise from oxygen defects. Furthermore, since the increase in the number of charge carriers does not lead to an increase of the spectral weight of the 235 meV peak, polarons can be ruled out as an explanation.

The intensity of the mode depends strongly on the light polarization (Fig. 4). In a cubic crystal, the Raman intensity for parallel and crossed polarizations can be expressed via E_g, T_{2g}, and A_{1g} symmetry components:

$$I_{\text{parallel}} = \left(\frac{2}{3} - a_\theta - b_\theta\right)E_g + (a_\theta + b_\theta)T_{2g} + \frac{1}{3}A_{1g},$$
$$I_{\text{crossed}} = b_\theta E_g + \left(\frac{1}{2} - b_\theta\right)T_{2g}, \quad (1)$$

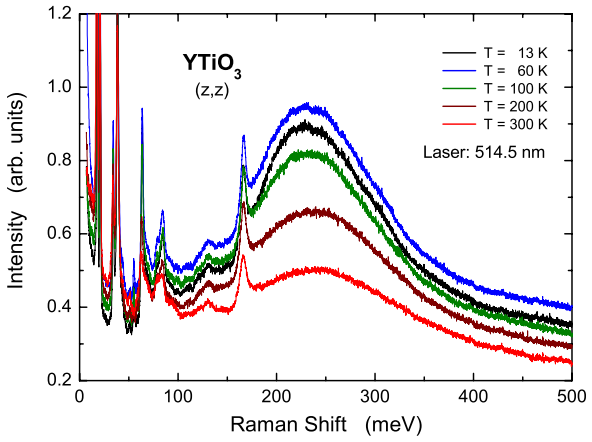

FIG. 3 (color online). Temperature dependence of the Raman spectrum of $YTiO_3$ in (z, z) geometry, using the 514.5 nm laser line.

where θ is the angle between the incident electric field vector and the c axis, $a_\theta = \frac{1}{2}\sin^2\theta$, $b_\theta = \frac{3}{8}\sin^2 2\theta$, and $\theta = 90°$ corresponds to the a (or b) axis. These relations provide a good description of the observed polarization dependences in both compounds (insets in Fig. 4).

We now turn to the interpretation of the 235 meV mode. Having ruled out phonons, luminescence, and oxygen defects, we attribute the mode to electronic scattering. Its line shape, temperature, and polarization dependence shows striking similarities (elaborated later on) with the Raman scattering from spin-pair excitations in the insulating parent compounds of the superconducting cuprates [24,25,27]. However, a simple two-magnon origin of this band is ruled out here because $YTiO_3$ is ferromagnetic, and because the peak energy is much higher than twice the magnon energies found by neutron scattering: ~20 meV in $YTiO_3$ [16] and ~44 meV in $LaTiO_3$ [15]. We thus attribute the broad Raman mode to the orbital degrees of freedom of the valence electron [28].

Let us start with a crystal field picture where the incident photon excites an oxygen $2p$ electron to unoccupied t_{2g} orbitals via the charge-transfer gap Δ_{pd} and, in a second step, the d electron in the ground state orbital relaxes to the oxygen site emitting a photon and leaving a "flipped" orbital behind. Predictions for the energy cost of such a local orbital flip vary between 27 and 240 meV [6,10,11], but some model calculations yield energies comparable to those observed experimentally [6,8]. The large width of the crystal field transitions can be understood as a consequence of coupling to lattice vibrations. Other aspects of the Raman data are, however, difficult to reconcile with a local crystal field scenario. First, the experimentally observed strong temperature dependence of the spectral weight is hard to understand within this picture, as the local pd charge-transfer process is not sensitive to temperature variations. Second, the above described scenario cannot explain the polarization dependence and the observed strong resonance at a photon energy of 2.54 eV, which is far below the pd-excitation energy $\Delta_{pd} > 4$ eV [29].

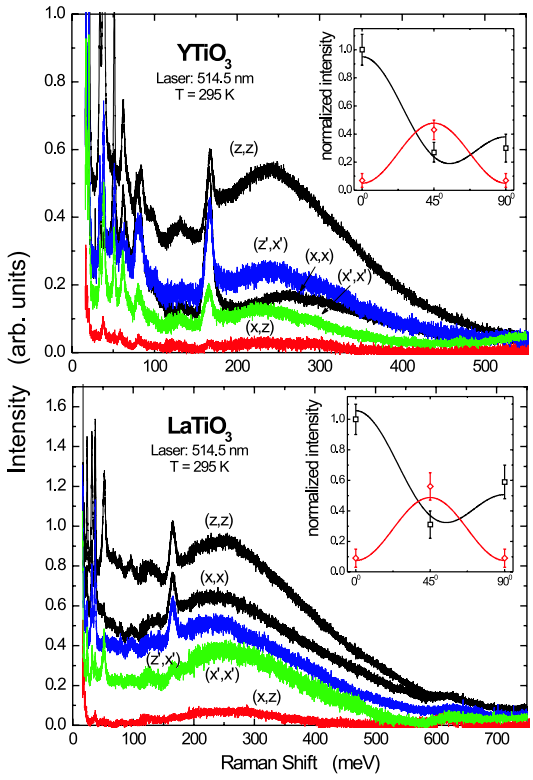

FIG. 4 (color online). Polarization dependences of the Raman spectra of $YTiO_3$ and $LaTiO_3$ at room temperature. The intensity is symmetric with respect to $(\alpha, \beta) \rightarrow (\beta, \alpha)$. A frequency independent background has been subtracted. Insets: scattering intensities for the parallel (□) and crossed (◇) polarizations as function of angle θ. Solid and dashed lines are obtained from Eq. (1), with relative intensities $E_g{:}A_{1g}{:}T_{2g} \approx 1{:}0.3{:}0.1$ (1:0.5:0.1) in $YTiO_3$ ($LaTiO_3$).

The resonance energy yields an important clue to the microscopic origin of the broad Raman peak. As it falls in the range of interside $d_i \rightarrow d_j$ excitations in optical spectra [29], *two* Ti sites must be involved in the Raman process. This means that the t_{2g} electron is first transferred to a neighboring site by the incident photon that matches the $d_i \rightarrow d_j$ transition energy. The intermediate state then relaxes back, leaving behind flipped orbitals either on one or on both sites, depending on the actual orbital pattern. Considering again the lattice-driven orbital picture, one finds that the orbital excitations probed by light polarized along different crystal axes are fundamentally different. In particular, the selection rules for the four-sublattice pattern $(xz \pm xy)/\sqrt{2}$, $(yz \pm xy)/\sqrt{2}$ suggested for $YTiO_3$ [9,12,14] allow a single orbital-flip for ab-plane polarization, but only two-orbiton excitations may occur in case of light polarization along the c axis [30]. This selection rule (which results from a mirror symmetry of the Ti-O-Ti bonds along the c axis) is in contrast to the observed polarization independence of the peak position.

In an alternative picture, proposed in Refs. [15–18], the orbitals are regarded as quantum objects much like the spins of the correlated electrons, and interact with each

other via the superexchange mechanism. Similar to the spin exchange (permutation) operator $\hat{P}_s = (2\vec{s}_i\vec{s}_j + \frac{1}{2}n_in_j)$, the orbital exchange is described by $\hat{P}_{\rm orb} = (2\vec{\tau}_i\vec{\tau}_j + \frac{1}{2}n_in_j)^{(\gamma)}$, where the action of pseudospins $\vec{\tau}^{(\gamma)}$ on the t_{2g} orbital triplet depends on the bond direction γ, leading to strong frustration of orbitals on a cubic lattice [17,18]. These frustrations, as well as the simultaneous spin/orbital exchange described by a product $\hat{P}_s\hat{P}_{\rm orb}$, result in a large degeneracy of competing many-body states, including the near-degeneracy of spin ferro- and antiferromagnetic states. The high-energy response of orbitals in titanates is governed by the universal scale $J_{\rm SE} \propto 4t^2/U_{dd}$ (*per bond*), controlled by the kinetic energy t and Hubbard correlation U_{dd}. Weak lattice distortions tend to polarize the many-body orbital state, but the high-energy orbital fluctuations respect the nearly cubic symmetry of the electronic ground state. This mechanism has also been invoked to explain the isotropic spin-wave spectra [15,16].

In the superexchange-driven orbital state of $YTiO_3$ [18], the light scattering from fluctuations of the *orbital-exchange* bonds, described by $\hat{P}_{\rm orb}$, leads to a two-orbiton Raman band of cubic E_g symmetry [31], as observed. The A_{1g} and T_{2g} components are explained due to next-nearest-neighbor orbital-exchange terms that are enhanced by resonant scattering, in complete analogy to the theory of magnetic Raman scattering in the cuprates [32]. From an analysis of the spin-wave data of Ref. [16], the highest orbiton energy was determined as $\sim 2r_1J_{\rm SE}$ with $r_1J_{\rm SE} \sim 60$ meV and $r_1 \sim 1.5$ [18], in reasonable agreement with a two-orbiton peak at the experimental value of 235 meV. Since the orbital excitations are strongly damped because of frustrating interactions, their response is broad in both momentum and energy, as observed.

In summary, we found orbital excitations in $LaTiO_3$ and $YTiO_3$ at approximately 235 meV. The superexchange-driven quantum orbital picture provides a consistent description of this observation as well as the polarization and temperature dependence of these excitations. In this picture, the high-energy Raman peak is due to light scattering from exchange-bond fluctuations, a process which is basically identical to magnetic Raman scattering in copper oxides. A pseudo-spin-like behavior of quantum orbitals explains why the Raman response of two apparently different degrees of freedom exhibit very similar features. In fact, the energies of the two-orbiton Raman mode in the titanates ($\sim$235 meV) and the two-magnon mode in the cuprates ($\sim$350 meV) are related by the simple scaling relation for the exchange-pair energy $\Omega_{\rm pair} \sim (z-1)J_{\rm SE}$, where $J_{\rm SE}$ and z are the strength and number of exchange bonds, respectively. These considerations, which can be readily extended to other transition metal compounds with more than one valence electron (or hole), provide a glimpse of an underlying universality in the electronic spectra of these complex materials.

We would like to thank M. Cardona, R. Zeyher, and R. Rückamp for useful discussions. The work is supported by the DFG through No. UL164/4 and in Cologne through No. SFB608.

[1] M. Imada, A. Fujimori, and Y. Tokura, Rev. Mod. Phys. **70**, 1039 (1998).
[2] Y. Tokura and N. Nagaosa, Science **288**, 462 (2000).
[3] E. Saitoh *et al.*, Nature (London) **410**, 180 (2001).
[4] M. Grüninger *et al.*, Nature (London) **418**, 39 (2002).
[5] E. Saitoh *et al.*, Nature (London) **418**, 40 (2002).
[6] M. Cwik *et al.*, Phys. Rev. B **68**, 060401(R) (2003).
[7] M. Mochizuki and M. Imada, Phys. Rev. Lett. **91**, 167203 (2003).
[8] R. Schmitz, O. Entin-Wohlman, A. Aharony, A. B. Harris, and E. Müller-Hartmann, Phys. Rev. B **71**, 144412 (2005).
[9] H. Sawada, N. Hamada, and K. Terakura, Physica (Amsterdam) **B237–238**, 46 (1997).
[10] I. V. Solovyev, Phys. Rev. B **69**, 134403 (2004).
[11] E. Pavarini *et al.*, Phys. Rev. Lett. **92**, 176403 (2004).
[12] M. Itoh, M. Tsuchiya, H. Tanaka, and K. Motoya, J. Phys. Soc. Jpn. **68**, 2783 (1999).
[13] T. Kiyama and M. Itoh, Phys. Rev. Lett. **91**, 167202 (2003).
[14] J. Akimitsu *et al.*, J. Phys. Soc. Jpn. **70**, 3475 (2001).
[15] B. Keimer *et al.*, Phys. Rev. Lett. **85**, 3946 (2000).
[16] C. Ulrich *et al.*, Phys. Rev. Lett. **89**, 167202 (2002).
[17] G. Khaliullin and S. Maekawa, Phys. Rev. Lett. **85**, 3950 (2000); G. Khaliullin, Phys. Rev. B **64**, 212405 (2001).
[18] G. Khaliullin and S. Okamoto, Phys. Rev. Lett. **89**, 167201 (2002); Phys. Rev. B **68**, 205109 (2003).
[19] E. D. Nelson, J. Y. Wong, and A. L. Schawlow, Phys. Rev. **156**, 298 (1967).
[20] M. Reedyk, D. A. Crandles, M. Cardona, J. D. Garrett, and J. E. Greedan, Phys. Rev. B **55**, 1442 (1997).
[21] M. N. Iliev *et al.*, Phys. Rev. B **69**, 172301 (2004).
[22] The Raman signals on polished and freshly cleaved surfaces are almost identical. Surface related defects can therefore be ruled out.
[23] C. Ulrich *et al.* (to be published).
[24] K. B. Lyons, P. A. Fleury, L. F. Schneemeyer, and J. V. Waszczak, Phys. Rev. Lett. **60**, 732 (1988).
[25] M. Yoshida *et al.*, Phys. Rev. B **46**, 6505 (1992).
[26] T. Katsufuji and Y. Tokura, Phys. Rev. B **49**, R4372 (1994).
[27] P. Knoll, C. Thomsen, M. Cardona, and P. Murugaraj, Phys. Rev. B **42**, R4842 (1990).
[28] The electronic origin is underlined by the observation of a similar broad structure in infrared transmission which has been attributed to a phonon-assisted orbital excitation, see R. Rückamp *et al.*, New J. Phys. **7**, 144 (2005).
[29] Y. Okimoto, T. Katsufuji, Y. Okada, T. Arima, and Y. Tokura, Phys. Rev. B **51**, 9581 (1995).
[30] S. Ishihara, Phys. Rev. B **69**, 075118 (2004).
[31] G. Khaliullin (to be published).
[32] B. S. Shastry and B. I. Shraiman, Phys. Rev. Lett. **65**, 1068 (1990).